Solid-State Extrusion of Isotactic Polypropylene Through a Tapered Die. I. Phenomenological Analysis

K. Nakamura[a]; K. Imada[a]; M. Takayanagi[a]

[a] Faculty of Engineering, Kyushu University, Fukuoka, Japan

PLEASE SCROLL DOWN FOR ARTICLE

Solid-State Extrusion of Isotactic Polypropylene Through a Tapered Die. I. Phenomenological Analysis

K. NAKAMURA,† K. IMADA and M. TAKAYANAGI

Faculty of Engineering, Kyushu University, Fukuoka, Japan

The solid state extrusion of isotactic polypropylene through a tapered die was conducted under various extrusion conditions using a piston-cylinder type extruder. The equation for evaluating the extrusion pressure was derived based on the plasticity theory as a function of die geometry and frictional coefficient between die wall and material. The integrand of the equation includes the yield stress as a function of true strain, which was given by the tensile properties of the same polymer. The data of lower degree of processing were fairly well described by the equation, but the estimation was not so accurate at high extrusion ratio. The molecular weight dependence of extrusion pressure was very small in solid state extrusion compared with the case of melt viscosity. This fact showed that the local intermolecular interaction is a predominant factor in solid state extrusion. The effect of frictional resistance on a cylinder part was found to be negligible in our experimental conditions.

INTRODUCTION

Recently cold and hot working of thermoplastics have drawn much attention not only of the investigators in the field of polymer science but also of the engineers who devote themselves to polymer processing. These processes are very interesting from the view point that it is unnecessary to melt the material in contrast to the traditional method composed of melting, injecting and cooling cycle. Rolling, forging, extrusion and deep drawing in a solid state are examples of this working method, and they have been developed along the ideas employed in the field of metal processing.

† Visiting researcher from the Central Research Laboratory, Sumitomo Chemical Industry Co. Ltd.

Imada *et al.*[1-3] have studied the extrusion of high density polyethylene (HDPE) and nylon-6 below their melting points. They analyzed the extrusion process by taking account of the fact that these crystalline polymers show remarkable strain hardening behavior and have derived the equation which could estimate the extrusion pressure for extrusion through a tapered die as a function of geometries of tapered die. The analysis of crystal orientation by wide angle X-ray scattering, the analysis of the super structure of the extrudate by small angle X-ray scattering and electron microscopic observation of the surface of extrudate were also made.[3,4] The crystal *c*-axis orientation in extruded product was very high along the extrusion direction and the appearance of the extrudate obtained with high degree of deformation was highly transparent and dimensionally stable against temperature rise.

Before us, Buckley[5] had tried the extrusion of many kinds of crystalline polymers such as low density polyethylene, HDPE, polypropylene (PP), nylon-66 and polyoxymethylene at room temperature. He reported the data on the extrusion pressure and the mechanical and physical properties of the extrudates. His processing was limited to the range of low degree of deformation as compared with the range covered by us. In this paper we will report on the extrusion of isotactic polypropylene below its melting point. The extrusion process of the polymer will be analyzed on the basis of the tensile properties of the same polymer at normal pressure according to the theorems of plasticity.

ESTIMATION OF EXTRUSION PRESSURE BASED ON THE SIMPLIFIED SCHEME OF PRESSURE BALANCE

1 Cylinder part

Figure 1 shows a hypothetical stress field of extrusion process of solid materials through a tapered die. The rod shaped material (the billet) having radius R is inserted into the cylinder with the same diameter and extruded through a tapered die of which inlet radius is R and outlet radius is r.

Equilibrium of the forces acting on a hypothetical disc having thickness dz in the cylindrical part indicated by (a) in Figure 1 is first considered. The static equilibrium is represented by

$$\pi R^2 \cdot d\sigma_z = 2\pi R \mu \sigma_r \cdot dz \qquad (1)$$

or

$$\frac{d\sigma_z}{\sigma_r} = \frac{2\mu}{R} dz \qquad (2)$$

where σ_z and σ_r are the stresses acting along axial and radial directions, respectively, and μ is the frictional coefficient between the material and the
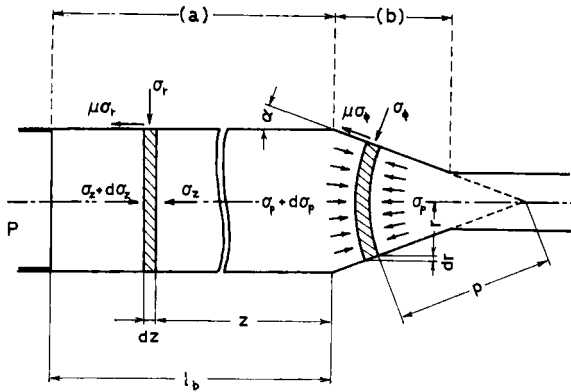
FIGURE 1 Schematic representation of stresses acting on the solid material being extruded through a tapered die. (a) cylinder part, (b) tapered die part.

inner wall of cylinder. It is assumed that the state of stress in this part is hydrostatic, that is, $\sigma_z = \sigma_r$, and Eq. (2) can be integrated as follows.

$$ln \frac{\sigma_z}{\sigma_{zo}} = \frac{2\mu}{R} z \tag{3}$$

where σ_{zo} is the stress at the entrance of the die ($z = 0$). Consequently the extrusion pressure P exerted at the end of billet is obtained as follows

$$P = P_o \exp\left(\frac{2\mu}{R} l_b\right) \tag{4}$$

where l_b is the length of undeformed part and P_o is the pressure at the entrance of the tapered die.

2 Tapered die part

Next the equilibrium of the forces in the tapered die part is considered. In part (b) in Figure 1 the stresses acting on an element of deformed part are indicated by the arrows. As to the state of stress in the tapered die part the following assumptions are made: (1) the state of stress is spherically symmetrical, and (2) the normal stresses σ_p and σ_ϕ are homogeneous in the elementary shell shown in part (b) of Figure 1. The subscript p is adopted here for denoting the radial direction instead of z, the axial direction of cylinder part in 1. σ_ϕ denotes the normal stress to the die wall. From the equilibrium of the forces along extrusion direction we obtain

$$(\sigma_p + d\sigma_p)\pi(r + dr)^2 = \sigma_p\pi r^2 + \sigma_\phi \cdot 2\pi r \cdot dr \, (\sin a + \mu \cos a)/\sin a \tag{5}$$

where α is the half-die angle and r is the radius of the circular cross-section which is obtained by projecting the spherical cone with radius p on the plane perpendicular to the axial direction as shown in part (b) of Figure 1. As used in the field of metal extrusion[6] true strain ϵ is defined by Eq. (6) and B is defined by Eq. (7).

$$\epsilon = ln\left(\frac{R}{r}\right)^2 \quad or \quad d\epsilon = -2\frac{dr}{r} \tag{6}$$

$$B = \mu \cot \alpha \tag{7}$$

Substitution of Eqs. (6) and (7) into Eq. (5) gives

$$\frac{d\sigma_p}{d\epsilon} = \sigma_p - \sigma_\phi \cdot (1 + B) \tag{8}$$

A relation between σ_p and σ_ϕ is associated with the yield criterion. The Tresca and Von Mises criteria give the same result, which is represented by Eq. (9).

$$Y(\epsilon) = \sigma_p - \sigma_\phi \quad (\sigma_\phi < \sigma_p < 0) \tag{9}$$

where $Y(\epsilon)$ is the yield stress of the material which undergoes deformation of strain ϵ in uniaxial tension. From Eqs. (8) and (9) we obtain

$$\frac{d\sigma_p}{d\epsilon} = (1 + B) \cdot Y(\epsilon) - B\sigma_p \tag{10}$$

Eq. (10) is a first-order linear differential equation and the following solution is obtained.

$$\sigma_p = -(1 + B)\int_0^\epsilon Y(\epsilon) \cdot \exp(B\epsilon) \cdot d\epsilon + \sigma_{po} \cdot \exp(B\epsilon) \tag{11}$$

where σ_{po} is the stress at the exit of the die. In this study σ_{po} can be eliminated as zero, since the material is extruded without tension at the exit of the die. Consequently the extrusion pressure at the entrance of the tapered die part P_o is represented as follows

$$P_o = (1 + B)\int_0^{2ln(R/r)} Y(\epsilon)\exp(B\epsilon)\,d\epsilon \tag{12}$$

If a functional form of $Y(\epsilon)$ is known, the value of P_o is calculated with the die geometries of R, r and α, and the frictional coefficient μ between die wall and material.

EXPERIMENTAL

1 Materials

Two types of commercial polypropylene, PP-A and PP-B, were used as the experimental materials. Table I lists some constants of the samples. Viscosity-average molecular weight $\overline{M}_v$ of these resins was determined by the solution viscosity by using the equation given by Parrini *et al.*[7]

TABLE I

Polypropylene samples used

Sample	M.I. (g/10 min)	$\overline{M}_v$	Density (g/cm³)	Crystallinity (%)
PP-A†	0.46	4.7×10^5	0.904	65
PP-B‡	7.90	2.7×10^5	0.907	68

† Sumitomo Noblen D501
‡ Sumitomo Noblen W101

Billets of these polymers for extrusion experiments were rods, the size of which is 9.9 mm in diameter and $25 \sim 40$ mm in length. They were prepared by cutting the discs with lathe, which had been molded by slow-cooling from the melt. The densities and the crystallinities of these billets at 25°C are also listed in Table I, where densities were measured by floatation method using water-ethanol system and crystallinities were estimated by assuming the densities of the crystalline and amorphous phase as 0.936[8] and 0.850 g/cm³,[8] respectively.

2 Extrusion device and extrusion method

The device used for extrusion experiments was a pison-cylinder type one, which was inserted between both plates of an oil press. Figure 2(a) shows it schematically. The outer and inner diameters of the cylinder were 84 mm and 10 mm, respectively. The die used had a shape as shown in (b) of Figure 2, the size of which is listed in Table II. The inlet diameter $2R$, the total length L and the half angle α of the die were fixed to be 10 mm, 15 mm and 20°, respectively, for all of the experiments. The outlet diameter $2r$ was selected among the values of 4, 5, 6 and 7 mm, in each experiment. The extrusion was conducted by direct extrusion method at constant temperatures higher than room temperature and below the melting point of the polymer. The extrusion load was applied by an oil press. The cylinder was heated with a ribbon heater wound around it and also with the hot plates of an oil press. The extrusion temperature was controlled within an accuracy of ± 1°C.
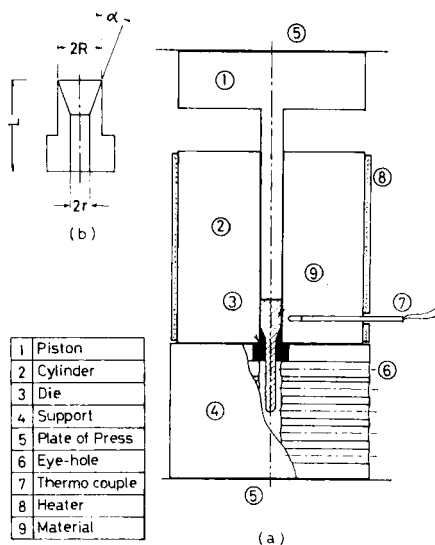
FIGURE 2   Schematic representation of extrusion device. (a) piston, cylinder and die assembly, (b) vertical section of die.

TABLE II

Size of dies employed in extrusion experiment

	Notation	Size
Inlet diameter	$2R$†	10 mm
Outlet diameter	$2r$	4, 5, 6, 7 mm
Total length	L	15 mm
Half die angle	α	20°

† Symbols are shown in the part (b) of Figure 2

After preheating the billet in the cylinder at the prescribed temperature for one hour the extrusion experiment was started by applying a constant pressure to the piston through the oil press. The length of the extrudate was measured from time to time through eyeholes in the support (cf. Figure 2).

To describe the degree of processing, the extrusion ratio $(R/r)^2$, that is, the ratio of cross-sectional areas of the inlet and the outlet part of the die was used.

3   Tensile stress–strain measurement

The true stress–true strain relationships of PP were measured by using a constant speed tensile testing machine with an air oven, Tensilon UTM-III

(Toyo Baldwin Co. Ltd.). The sample was prepared by annealing a quenched sheet at 120°C for half an hour. The specimen size was about 4 mm wide and 0.5 mm thick and the distance between the ends of the specimen holders of the tester was 20 mm. After preheating the specimen at the prescribed temperature for 30 minutes, the test was conducted at constant crosshead speed of 5 mm/min (25%/min).

The true stress–true strain relations of PP cannot be obtained easily from the conventional stress–strain curves because a necking phenomenon is observed at few percent extension. We therefore estimated approximately true stress σ and true strain ϵ by the following procedure. Midway during tensile testing the extension was stopped, and the cross-sectional area S of the drawn sample was measured after removing the specimen from the tester. σ and ϵ were calculated by Eqs. (13) and (14) by using the values of F, S and S_o.

$$\sigma = \frac{F}{S} \tag{13}$$

$$\epsilon = \int_{l_o}^{l} \frac{dl}{l} = ln\left(\frac{l}{l_o}\right) = ln\left(\frac{S_o}{S}\right) \tag{14}$$

where F is the load measured with testing machine just before removing the specimen from the tester and S_o is the initial cross-sectional area of the specimen.

RESULTS AND DISCUSSION

1   Tensile behavior

Figure 3(a) and 3(b) show the true stress–true strain relations of PP-A and PP-B, respectively, at various temperatures. These data show that true stress increases rapidly with increasing true strain, especially in high strain region. Thus, remarkable strain hardening phenomenon is recognized in PP as found in the cases of HDPE and nylon-6, for which it has already been reported by us[9] that the true stress–true strain relations for these polymers can be expressed by the equation in a generalized form as Eq. (15).

$$log(\sigma/\sigma^*) \cdot log(\epsilon/\epsilon^*) = -c \tag{15}$$

where σ^* and ϵ^* are the constants depending on the grade and species of polymers, drawing temperature, strain rate and composition of the blend. The constant c depends only on the polymer species, the values of which are 0.384 and 0.175 for HDPE and nylon-6, respectively. This generalized
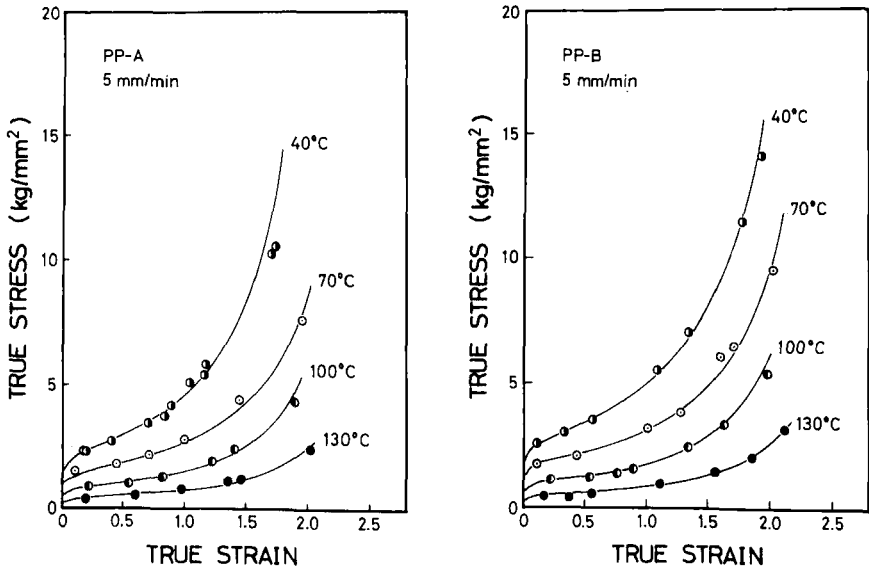
FIGURE 3 True stress v. true strain curves at various temperatures (a) for PP-A and (b) for PP-B. Solid lines show the calculated values by using Eq. (15) with the values of c, σ^* and ϵ^* listed in Table III.

correlation has also been confirmed for PP in the present study. The values of c, σ^* and ϵ^* for PP, which were determined by trial and error method by shifting the logarithmic data along both axes, are listed in Table III. The value of c was constantly 0.23 throughout the whole experiments. It was confirmed again that the value of c is characteristic of PP, being independent of the molecular weight of the sample or test temperatures or draw speeds. The

TABLE III

The values of c, σ^* and ϵ^* of PP-A and PP-B drawn at various temperatures

Sample	Temperature (°C)	c	σ^* (kg/mm²)	ϵ^*
PP-A	40	0.23	1.55	3.1
	70	0.23	1.00	3.5
	100	0.23	0.55	3.35
	130	0.23	0.295	3.55
PP-B	40	0.23	1.82	3.45
	70	0.23	1.20	3.6
	100	0.23	0.65	3.45
	130	0.23	0.34	3.65

value of σ^* decreases with increasing temperature, while ϵ^* seems to be almost insensitive to temperature. These tendencies are the same as found in the cases of HDPE and nylon-6. Some molecular weight dependence is noticed in σ^*, that is, the lower molecular weight sample of PP-B shows higher σ^* value than the higher molecular weight PP-A. In Figures 3(a) and 3(b) σ–ϵ curves calculated from Eq. (15) by using the values of c, σ^* and ϵ^* listed in Table III are also shown by solid lines, which are in good agreement with experimental values. In the calculation of extrusion pressure mentioned in the following section, these calculated values were used. Figure 4 shows a composite curve obtained by shifting both logarithmic curves of σ and ϵ measured at various conditions.
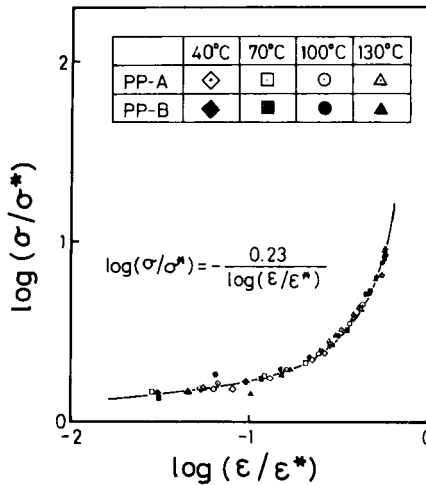
FIGURE 4 A composite curve of $\log(\sigma/\sigma^*)$ v. $\log(\epsilon/\epsilon^*)$ for PP. Solid line is calculated according to Eq. (15) using the values of c listed in Table III.

2 Extrusion behavior

An example of extrusion behavior at constant pressure is shown in Figure 5 (for PP-A at 40°C with $(R/r)^2 = 2.8$). It was found that the extrusion curves are composed of the beginning part of transient rapid extrusion and the part of steady state extrusion. Figure 6 shows plot of the extrusion rate determined by the slope of steady state extrusion against pressure. In each curve of Figure 6 the pressure at which the extrusion rate abruptly increases can be found and we define this critical pressure as extrusion pressure.

3 Effect of undeformed part in the cylinder

Figure 7 shows the effect of initial length of billet l_{bi} on extrusion pressure. This effect is found to be very small. According to Eq. (4) the relation between
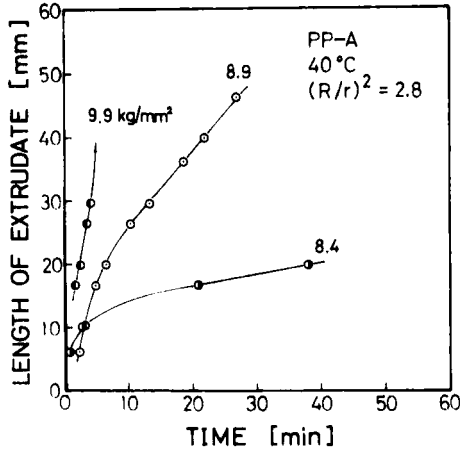
FIGURE 5   Extrusion process of PP-A under various pressures at 40°C. Extrusion ratio is 2.8.
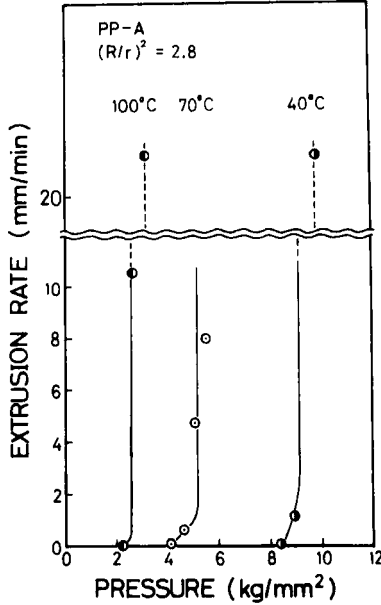

FIGURE 6   Extrusion rate v. pressure for PP-A at various temperatures. Extrusion ratio is 2.8.
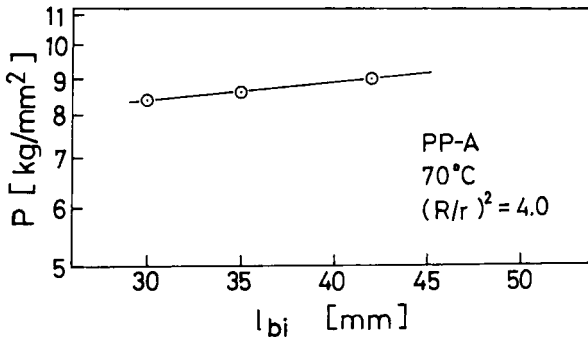
FIGURE 7 Extrusion pressure v. initial billet length l_{bi} for PP-A at 70°C. Extrusion ratio is 4.0.

log P and l_{bi} is expected to be linear and the slope of straight line gives the frictional coefficient, μ, between the material and the inner wall of cylinder. The estimation of μ from the data shown in Figure 7 gives a very small value about 0.01. This small value of frictional coefficient may allow the assumption that the effect of friction at the undeformed part is so small that it is negligible in estimating extrusion pressure. In the analysis described below such an assumption was adopted.

4 Effects of extrusion ratio and temperature on extrusion pressure

Figure 8 shows the relationships between extrusion pressure and the extrusion ratio at various temperatures. The solid lines in Figure 8 represent the extrusion pressure calculated by using Eq. (12) with substitution of tensile data of the same polymer. The value of μ was determined to be 0.30 by a trial and error method so as to satisfy the observed values. This value of μ agreed well with the frictional coefficient of $0.3 \sim 0.4$ between PP and steel in the literature.[10] It is noticed in Figure 8 that the calculated values in high extrusion ratio at 70, 100 and 130°C are much smaller than the observed values. Tensile properties used to calculate the extrusion pressure in Eq. (12) were measured at atmospheric pressure. If we take into account the fact that the yield stress of PP in uniaxial deformation largely increases with increasing hydrostatic pressure,[11] the large deviation of experimental data from the calculated values in high extrusion ratio can be considered to be due to the pressure dependence of yield stress of PP.

The value of frictional coefficient $\mu = 0.30$ in a tapered part of the die is much different from that of the undeformed part, $\mu = 0.01$ in the cylinder part. Such large difference of frictional coefficients determined experimentally might lead us to the consideration that the state of stress in the cylinder part
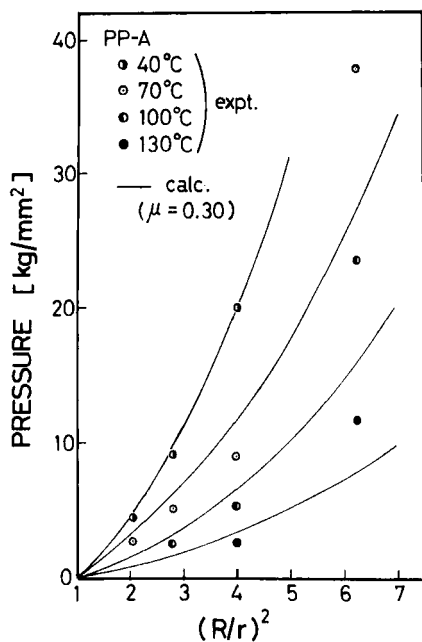
FIGURE 8 The extrusion ratio dependence of extrusion pressure at various temperatures for PP-A. Solid lines show the calculated values of extrusion pressure by using Eq. (12).

is not hydrostatic as assumed in **1**, that is, σ_r is not equal to σ_z and far less than that. Figure 9 shows the temperature dependence of extrusion pressure at several extrusion ratios as indicated in the figure. The extrusion pressure rapidly decreases with increasing temperature, and the curves seem to be extrapolated to intersect the abscissa at the melting point of PP, 165°C. Such tendencies are very acceptable to us, if we consider that the yield behavior of solid crystalline polymers disappears at the melting temperature, where the crystallinity disappears completely.

Appearance of extrudates is shown in Figure 10. The extrudates at high extrusion ratio are extraordinarily transparent. The surface of extrudates, however, becomes rough as the extrusion ratio increases, and the extrudates at extrusion ratio of 6.3 showed the shark skin like surface. At further high extrusion ratio such as 8.3, cracks were produced in the extrudates, and stable extrusion as shown in Figure 5 could not be observed. The extrudates at extrusion ratio of 4.0 have good transparency and smooth surface. Among the samples at the same extrusion ratio 4.0, the transparency of the extrudates obtained at 70 and 100°C was better than that of those obtained at 40 and 130°C. Previously Takayanagi et al.[12] reported in the study of uniaxial stretching of PP that the best condition of drawing to obtain the highest
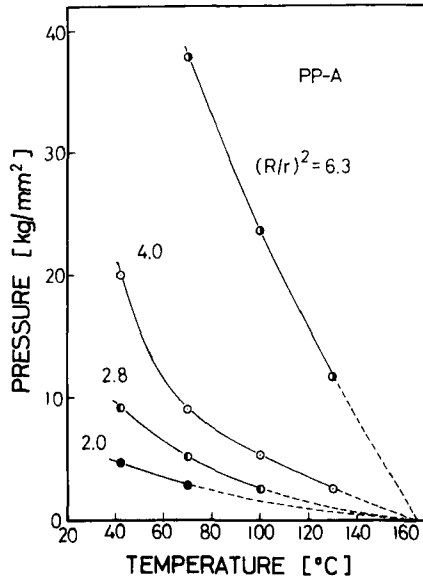
FIGURE 9 The temperature dependence of extrusion pressure for various extrusion ratio for PP-A.

degree of orientation, modulus value and ultimate strength is to conduct the drawing of bulk sample at the crystalline absorption temperature of PP, the maximum of which is located at 110°C at 110 Hz. This crystalline absorption temperature agreed well with the temperature at which the solid state extrusion proceeds smoothly to give the extrudates with highest transparency. This relation can be explained by the understanding that the lamellar crystals deform most efficiently at the crystalline absorption temperature, being scarcely accompanied by thermal distortion at higher temperature or local fracture at lower temperature. At this temperature, lamellar crystals become viscoelastic from purely elastic.[13] This phenomenon is comparable to that found in glassy polymer at its glass transition temperature, T_g. Drawing of the glassy polymer at T_g is widely known to give the highest orientation, modulus and strength.

The extrudates showed a slight tendency of die swell. The amount of die swell tended to increase with increasing extrusion rate. The amount of die swell of the extrudates, of which extrusion rate is higher than 5 mm/min, are listed in Table IV. The data are represented by $((r'-r)/r) \times 100$ (%), where r' is the radius of extrudate and r is the outlet radius of the die. The values are given for those measured just after extrusion and those for more than one month lapse after extrusion. The data further show that the amount of die swell at higher temperature extrusion is less even if the shrinkage due to the
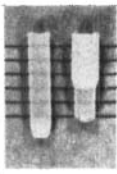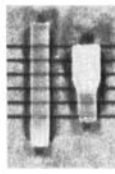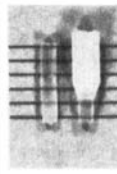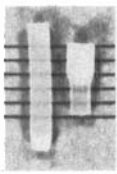
G

PP-A
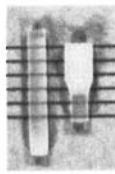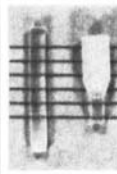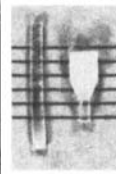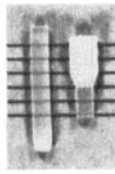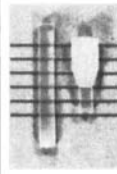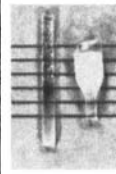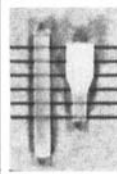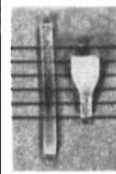
$(R/r)^2$	2.0	2.8	4.0	6.3
40°C				
70°C				
100°C				
130°C				

FIGURE 10   The appearance of extrudates under various conditions.

cooling effect from extrusion temperature to room temperature is corrected. The residual stress for elastic recovery or spring back might be removed at around the crystalline absorption temperature, where the most effective orientation is realized. More detailed discussion on the super-structure of the extrudate will be made in the following paper.

TABLE IV

The amount of die swell of PP-A and PP-B under various extrusion ratios and temperatures. The data in upper row are the values measured after one month lapse after extrusion, and the lower in the parentheses measured just after extrusion.

Sample	$(R/r)^2$	Die swell (%)			
		40°C	70°C	100°C	130°C
PP-A	2.0	11.1	10.1		
		(10.0)	(10.1)		
	2.8	11.7	11.2	10.5	
		(10.3)	(10.8)	(9.8)	
	4.0		11.0	8.4	6.0
			(10.6)	(8.2)	(6.0)
PP-B	4.0	8.2	5.4	4.6	1.8
		(7.4)	(5.6)	(4.8)	(2.2)

5 Effect of molecular weight

Figure 11 shows the true stress–true strain relationships for two types of PP, which are different in molecular weight as listed in Table I. In the range of strain covered in Figure 11 lower molecular weight sample PP-B (broken line) had higher yield stress compared with PP-A of higher molecular weight
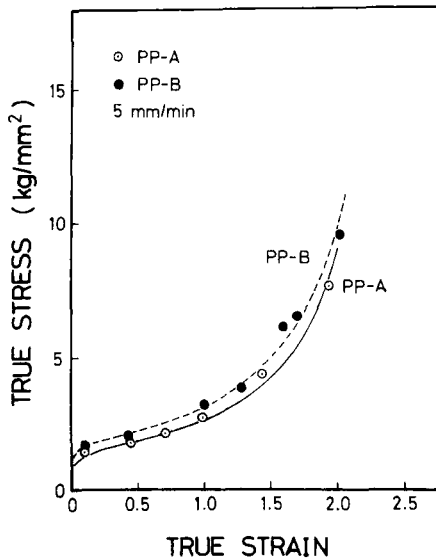

FIGURE 11   True stress v. true strain curves at 70°C for PP-A (open circles) and for PP-B (filled circles). Solid and broken lines show the calculated values by using Eq. (15) for PP-A and for PP-B, respectively.

(solid line). According to the phenomenological analysis conducted here by us, the extrusion pressure reflects the tensile property of the polymer, which predicts that the higher extrusion pressure will be necessary to extrude the lower molecular weight PP-B sample. Figure 12 shows the extrusion ratio
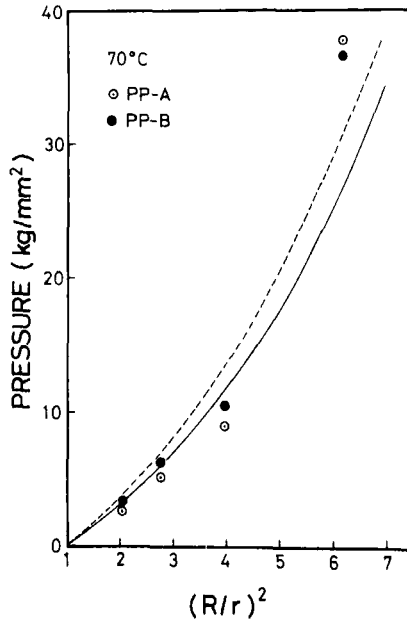

FIGURE 12   Extrusion pressure of PP-A (open circles) and PP-B (filled circles) for various extrusion ratios. Solid and broken lines show the calculated values by using Eq. (12) for PP-A and for PP-B, respectively.

dependence of extrusion pressure of PP-A (solid line) and PP-B (broken line) at 70°C, where the solid and broken lines are the calculated curves by using Eq. (12) and $\mu = 0.30$. Except the data at extrusion ratio of 6.3, the result of Figure 12 reflects the data of Figure 11. Figure 13 shows the temperature dependence of extrusion pressure of PP-A and PP-B at constant extrusion ratio (= 4.0). They also reflect the tensile properties of both polymers. The amount of die swell of PP-B is less than that of PP-A as seen in Table IV. The appearance of extrudates and limiting extrusion ratio of PP-B does not seem to be different from PP-A. From these results we recognize that the effect of molecular weight on the extrusion pressure in solid state extrusion is much smaller than that predicted in melt viscosity. In the latter case the flow resistance is largely affected by the entanglement between molecular chains as shown by the 3.4 power law of molecular weight dependence. On the other
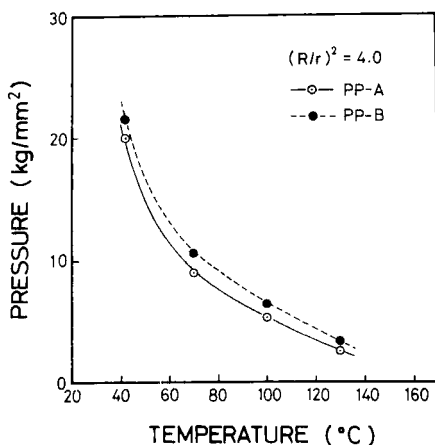
FIGURE 13   Extrusion pressure v. extrusion temperature for PP-A (open circles and solid line) and for PP-B (filled circles and broken line) at extrusion ratio 4.0.

hand, in the case of plastic deformation such as solid state extrusion it may be said that the short distance frictional factor between the molecular segments is a governing factor. Thus a molecular weight dependence as seen in melt viscosity cannot be observed. The fact that PP-B needs higher drawing stress or higher extrusion pressure than PP-A as shown in Figure 11, 12 and 13 will be due to the slightly higher crystallinity of lower molecular weight sample PP-B as listed in Table I.

CONCLUSION

The solid state extrusion of isotactic polypropylene was conducted under various extrusion conditions and the following results were obtained.

1   Isotactic polypropylene could be extruded easily at temperatures higher than room temperature and below the melting point. The extrudates obtained were transparent. To obtain a sample with best performance, the crystalline absorption temperature at about 110°C was most appropriate.

2   The equation derived by using the plasticity theory could estimate the extrusion pressure of PP as in the case of HDPE, although the estimation was not so accurate in high extrusion ratio as in the case of HDPE.

3   Frictional coefficients in the cylinder part and the tapered part in die were evaluated as $\mu = 0.01$ and 0.30, respectively.

4   The effect of molecular weight on the extrusion pressure in solid state extrusion was small. This phenomenon was predicted by the tensile data of

both samples, which are different in yield stress. Its reason seems to be ascribed to the slight difference in crystallinity between both samples.

References

1. K. Imada and M. Takayanagi, paper entitled "Plastic Deformation of High Density Polyethylene in Solid-State Extrusion" in preparation.
2. S. Maruyama, K. Imada, and M. Takayanagi, paper entitled "Further Studies on Solid-State Extrusion of Linear Polyethylene and its Blends with n-Paraffin" in preparation.
3. K. Imada, Y. Kondo, K. Kanekiyo, and M. Takayanagi, *RPPPJ.* **14**, 393 (1971).
4. K. Imada, T. Yamamoto, K. Shigematsu, and M. Takayanagi, *J. Material Sci.* **6**, 537 (1971).
5. A. Buckley and H. A. Long, *Polymer Eng. Sci.* **9**, 115 (1969).
6. G. E. Dieter, Jr., *Mechanical Metallurgy*, McGraw-Hill, New York (1961).
7. P. Parrini, F. Sebastiano, and G. Messina, *Makromol. Chem.* **38**, 27 (1960).
8. G. Natta, P. Corradini, and M. Cesari, *Atti. accad. nazl. Lincei, Rend. classe sci. fis. mat. e nat.* **22**, 11 (1957).
9. S. Maruyama, K. Imada, and M. Takayanagi, *Int. J. Polymeric Materials* **1**, 211 (1972).
10. R. B. Gregory, *SPE J.* **25**, 55 (Oct., 1969).
11. K. D. Pae, D. R. Mears, and J. A. Sauer, *J. Polymer Sci.*, Pt. B, **6**, 773 (1968).
12. M. Takayanagi, S. Minami, and H. Nagatoshi, Reports of the Association for Advancement of Engineering of Asahi Glass Company, **7**, 127 (1961).
13. M. Takayanagi, T. Aramaki, M. Yoshino, and K. Hoashi, *J. Polymer Sci.* **46**, 531 (1960).